



# Ellagic acid prevents dementia through modulation of PI3-kinase-endothelial nitric oxide synthase signalling in streptozotocin-treated rats

Manish Kumar<sup>1,2</sup> · Nitin Bansal<sup>2</sup>

Received: 25 February 2018 / Accepted: 7 June 2018 / Published online: 15 June 2018  
© Springer-Verlag GmbH Germany, part of Springer Nature 2018

## Abstract

Ellagic acid (EGA)-enriched dietary supplements are widely acclaimed, owing to its versatile bioactivities. Previously, we reported that chronic administration of EGA prevented the impairment of cognitive abilities in rats using the intracerebroventricular-administered streptozotocin (STZ-ICV) model of Alzheimer's disease. Impairment of phosphoinositide 3 (PI3)-kinase-regulated endothelial nitric oxide synthase (eNOS) activity by central administration of STZ in rodents instigates dementia. The aim of the present study was to delineate the role of PI3-kinase-eNOS activity in the prevention of STZ-ICV-induced memory dysfunctions by EGA. The Morris water maze and elevated plus maze tests were conducted, and brain oxidative stress markers (TBARS, GSH, SOD, CAT), nitrite, acetylcholinesterase (AChE), LDH, TNF- $\alpha$  and eNOS were quantified. Administration of EGA (35 mg/kg, p.o.) for 4 weeks daily attenuated the STZ-ICV (3 mg/kg)-triggered increase of brain oxidative stress, nitrite and TNF- $\alpha$  levels; AChE and LDH activity; and decline of brain eNOS activity. The memory restoration by EGA in STZ-ICV-treated rats was conspicuously impaired by *N*<sup>(G)</sup>-nitro-L-arginine methyl ester (L-NAME) (20 mg/kg, 28 days) and wortmannin (5  $\mu$ g/rat; ICV) treatments. Wortmannin (PI3-kinase inhibitor) and L-NAME groups manifested elevated brain oxidative stress, TNF- $\alpha$  content and AChE and LDH activity and diminished nitrite content. L-NAME (arginine-based competitive eNOS inhibitor) enhanced the eNOS expression (not activity) whereas wortmannin reduced the brain eNOS levels in EGA- and STZ-ICV-treated rats. However, the L-NAME group exhibited superior cognitive abilities in comparison to the wortmannin group. It can be concluded that EGA averted the memory deficits by precluding the STZ-ICV-induced loss of PI3-kinase-eNOS signalling in the brain of rats.

**Keywords** Ellagic acid · PI3-kinase-endothelial nitric oxide synthase (eNOS) · Memory · Wortmannin · Streptozotocin · Acetylcholinesterase

## Introduction

The lipid (e.g. glycerophospholipids, sphingolipids, eicosanoids)-mediated intracellular signalling plays a key role in inflammatory, proliferative and several metabolic disorders. Phosphoinositide 3-kinase (PI3-kinase) constitutes a subfamily of diverse lipid kinases that phosphorylates a 3'-hydroxyl group of phosphatidylinositols (PIs) to generate second

messengers such as PI(3)P, PI(3,4)P<sub>2</sub> and PI(3,4,5)P<sub>3</sub> that are recognised by proteins (e.g. Akt) having pleckstrin homology (PH) domains and thereby regulate cellular energy status (e.g. GSK-3), fatty acid synthesis, apoptosis (e.g. CREB, Bax, Bcl2, Bim), cell proliferation, cell cycle (e.g. FOXO), nitric oxide signalling (e.g. endothelial nitric oxide synthase (eNOS)) and several transcription factors (Franke 2008). PI3-kinase crosstalk with several other pathways such as TLR, JAK/STAT, VEGF, MAPK, p53 and chemokine signalling under the influence of plethora of bioactive molecules, notable ones are insulin, cytokines, neurotrophic factors (e.g. NGF) and microbial products (PAMPs), affects several brain processes including memory (Vivanco and Sawyers 2002). The anti-apoptotic and pro-survival activities of PI3-kinase are found reasonably beneficial in Alzheimer's disease (AD)

✉ Nitin Bansal  
nitindsp@rediffmail.com

<sup>1</sup> IKG Punjab Technical University, Kapurthala, Punjab 144603, India

<sup>2</sup> Department of Pharmacology, ASBASJSM College of Pharmacy, Bela, Ropar 140111, India

as progressive neurodegeneration, synaptic dysfunction and severe cognitive decline are manifested in advanced stages of AD-affected brain commensurate with hastened brain aging (Kong et al. 2013; Franke 2008). Preclinical studies have proclaimed that deregulation of PI3-kinase pathway spurs mitochondrial free radical yield and release of pro-inflammatory cytokines that embodies the basis of early neurodegenerative changes in AD pathology (Meng et al. 2017).

Central PI3-kinase dysfunction is known to induce tau phosphorylation (pTau) and aggravate amyloid  $\beta$  ( $A\beta$ ) toxicity by enhancing sequential amyloidogenic processing of amyloid precursor protein (APP) by  $\beta$ -secretase and  $\gamma$ -secretase in the brain (Baki et al. 2004; Petanceska and Gandy 1999). eNOS is a downstream target of PI3-kinase signalling involved in cognitive functions of the brain (Austin et al. 2013). Several studies corroborated eNOS hypoactivity-incited alterations in the brain akin to AD-type dementia (Austin et al. 2013; Provias and Jaynes 2008). Central administration of PI3-kinase inhibitors (e.g. LY294002 or wortmannin) interferes with eNOS functions and thereby aggravates AD symptoms in rodents (Agrawal et al. 2011; Petanceska and Gandy 1999). In central disorders, crosstalk between neuronal and endothelial NOS isoforms to restore nitric oxide (NO) transmission renders intact eNOS activity highly essential (Rickard et al. 1999; Son et al. 1996). Furthermore, PI3-kinase-eNOS signalling is associated with the brain cholinergic activity adversely affected in AD patients (Tyagi et al. 2010). In AD therapeutics, several drugs reinstating the brain cholinergic transmission (e.g. donepezil, rivastigmine) are in contemporary use that afford symptomatic relief in patients of dementia and is testimonial to the significance of acetylcholine in memory processes.

Ellagic acid (EGA) and ellagitannins (ETs) constitute natural polyphenols present in nuts, pomegranates, berries and wines and possess potent antioxidative, anti-inflammatory, vasorelaxant, hypolipidemic, antidiabetic and antitumor activities. Ellagic acid is classified as nutraceutical, owing to its significant health-promoting bioactivities which prompted emergence and wide consumption of commercially available EGA-enriched extracts such as Ellagic Active<sup>®</sup> tablets, PomActiv<sup>™</sup> and Biotech Nutritions Ellagic Acid Capsules<sup>®</sup> as dietary supplement (Lipinska et al. 2014). ETs are complex derivatives of hexahydroxydiphenolic acid and in vivo undergo spontaneous lactonisation to EGA which is a dimeric gallic acid derivative predominantly absorbed from the upper gastrointestinal tract. Preclinical and clinical studies revealed tissue deposits of urolithins (prostrate and intestine) and significant amounts of unchanged EGA in plasma, urine and faeces after consumption of EGA extract (Landete 2011; Yoshida et al. 2010).

Cerebral ischemia and many neurotoxins (e.g. streptozotocin, 1-methyl-4-phenyl-1,2,3,6-tetrahydropyridine) compromise PI3-kinase-mediated eNOS phosphorylation in the brain of rodents

and thereby incite synaptic dysfunction and profound cognitive decline (Rajasekar et al. 2017). The diabetogenic, pro-inflammatory and cytotoxic properties of streptozotocin (STZ) precipitate tauopathy and amyloidogenesis and instigate AD traits in the brain of rats (Lee et al. 2016). Revitalisation of PI3-kinase-eNOS activity is known to forbid the cognitive debility in STZ-treated rodents (Utkan et al. 2015). Many evidences have unveiled the anti-apoptotic and anti-inflammatory effects of EGA through modulation of PI3-kinase-eNOS signalling (Ou et al. 2010). Neuroprotective action of EGA against  $A\beta_{25-35}$ , STZ and traumatic brain injury (TBI) has been demonstrated in animal studies (Bansal et al. 2017; Kiasalari et al. 2017). EGA is able to restore endothelial dysfunction in mice and memory deficits in scopolamine- and diazepam-treated rats (Ding et al. 2014; Mansouri et al. 2016). However, the molecular insight into neuroprotective activity of EGA has been still eluded so far. Hence, the aim of the present study is to delineate the role of PI3-kinase-eNOS signalling in EGA-induced memory improvement in rats treated with intracerebroventricular streptozotocin (STZ-ICV).

## Materials and methods

### Drugs

Ellagic acid (HiMedia Laboratories, Mumbai) was suspended in 0.1% gum acacia maintaining the temperature  $45 \pm 5$  °C and pH 6–8 (Bansal et al. 2017). A 5% dimethyl sulphoxide (DMSO) in aCSF [147 mM NaCl (0.0859 g), 2.9 mM KCl (0.00216 g), 1.6 mM  $MgCl_2$  (0.00152 g), 1.7 mM  $CaCl_2$  (0.00249 g), 2.2 mM dextrose (0.00396 g) in 10 ml of water for injection (pH 7.3)] solution was used as vehicle for intracerebroventricular (ICV-vehicle) administration of streptozotocin (SRL Pvt., Ltd., Mumbai) and wortmannin (Sigma-Aldrich).  $N^{(G)}$ -Nitro-L-arginine methyl ester (Sigma-Aldrich) was dissolved in normal saline. All the drug solutions were freshly prepared before administration.

### Experimental animals and drug treatments

Wistar rats (180–220 g, either sex) were procured from the Central Animal Facility, All India Institute of Medical Sciences, New Delhi, and were reared at the Central Animal Facility of the institute under standard laboratory conditions (temperature,  $23 \pm 2$  °C; humidity,  $40 \pm 10\%$ ; natural light-dark cycle, 12 h each). The experimental protocol of this study was approved by the Institutional Animal Ethics Committee of the institute, and all procedures followed were as per guidelines of CPCSEA, Ministry of Forests and Environment, Government of India. Three rats per cage ( $44 \times 29 \times 16$  cm<sup>3</sup>) were housed and nurtured with standard rodent pellet diet (Ashirwad Industries, Mohali) and water ad libitum. The animals were acclimatised 2 weeks before experiments and

indiscriminately distributed to five different groups ( $n = 6$ ): (i) control group (Sham-treated) rats were administered ICV-vehicle (10  $\mu$ l); (ii) STZ group (STZ-ICV) rats were given streptozotocin (3 mg/kg, 10  $\mu$ l ICV-vehicle) alone; (iii) EGA+STZ group (EGA+STZ) was administered EGA (35 mg/kg, p.o.) for 4 weeks daily and STZ-ICV (3 mg/kg, 10  $\mu$ l ICV-vehicle); (iv) wortmannin group (EGA+STZ+Wort) received EGA (35 mg/kg, p.o.), STZ (3 mg/kg, 8  $\mu$ l ICV-vehicle) and wortmannin (5  $\mu$ g/rat in two divided doses, 2.5  $\mu$ g in 2  $\mu$ l ICV-vehicle); and (v)  $N^{(G)}$ -nitro-L-arginine methyl ester (L-NAME) group (L-NAME+EGA+STZ) received L-NAME (20 mg/kg, i.p.), EGA (35 mg/kg, p.o.) and STZ-ICV (3 mg/kg, 10  $\mu$ l ICV-vehicle).

EGA (35 mg/kg) was administered orally (10 ml/kg b.w.) for 4 weeks daily (Bansal et al. 2017). Rat brain surgery was performed after EGA treatment, and STZ was administered through ICV route on days 1 and 3 to trigger AD-type dementia. The modulation of PI3-kinase-regulated eNOS activity by EGA was elucidated by administering wortmannin (5  $\mu$ g/rat) through ICV route in STZ-ICV-treated rats. Previous studies depicted that central administration of wortmannin (0.5 ng–2.5  $\mu$ g per rat) irreversibly inhibits the PI3-kinase activity ( $IC_{50}$  value, 4–9 nM for PI3-kinase subunits) (Chen et al. 2012). L-NAME potently inhibits the eNOS and was injected (dose 20 mg/kg, i.p., 2 ml/kg in normal saline) (Traystman et al. 1995) in EGA- and STZ-ICV-treated rats for 4 weeks daily to explore the role of eNOS (Fig. 1). Normal saline (2 ml/kg) was administered to all remaining groups for 4 weeks daily.

### Surgery of the rat brain

For ICV administration, the rat was rendered insensitive before surgery by administering chloral hydrate (350 mg/kg, i.p.). The body of anaesthetised rat was placed on warm pad, and the head was positioned in the stereotaxic frame (INCO, Ambala, India). A mid-sagittal incision was made in the scalp, skin was retracted and skull was exposed. A burr hole was drilled through the parietal bone of the skull to access a randomly selected lateral cerebral ventricle (stereotaxic coordinates: antero-posterior from the bregma =  $-0.8$  mm,

mediolateral from the mid-sagittal suture =  $\pm 1.5$  mm, dorso-ventral from the skull =  $\pm 3.6$  mm) (Paxinos et al. 1980). On day 1, STZ (dose 3 mg/kg in 10  $\mu$ l ICV-vehicle) was slowly injected in the lateral cerebral ventricle of rats over a 10-min duration (1  $\mu$ l/min) (Sharma et al. 2010). After injection, the microneedle was not displaced for 5 min to enhance diffusivity of drug in CSF. The wortmannin group received STZ (3 mg/kg in 8  $\mu$ l ICV-vehicle) pursued by wortmannin (2.5  $\mu$ g in 2  $\mu$ l ICV-vehicle) (Gao et al. 2014; Yang et al. 2016). Hamilton<sup>®</sup> microsyringe was changed between different administrations without displacing the microneedle. Sham rats received the same volume (10  $\mu$ l) of ICV-vehicle only. The holes were repaired with dental cement post drug treatments, skin was sutured and Neosporin<sup>®</sup> was applied *pro re nata* to prevent contamination. The ICV administrations were repeated in the remaining lateral ventricle once after 48 h. Cefazolin sodium (Ranbaxy) was injected (30 mg/kg, i.p.) once postoperatively to avoid sepsis. Post-surgical hypothermia was prevented by keeping the rats warm ( $37 \pm 0.5$  °C). Post surgery, each rat was placed individually in separate cage ( $30 \times 23 \times 14$  cm<sup>3</sup>) for 7 days, allowing access to food and water gratis.

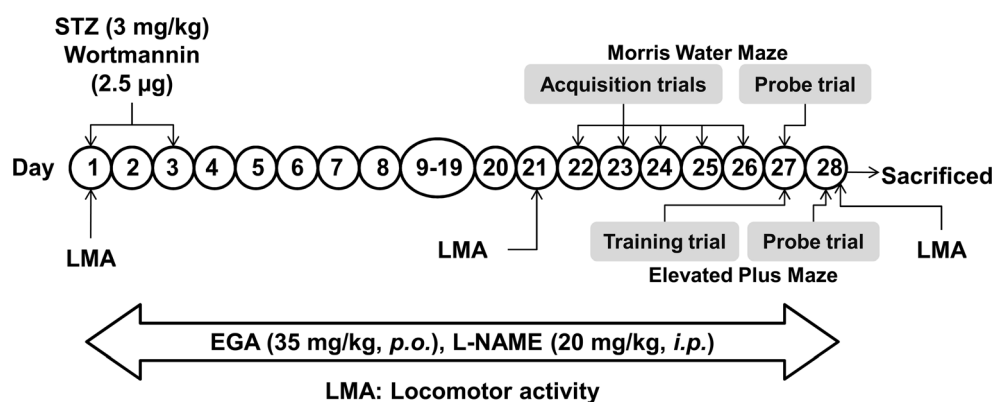
### Locomotor activity

The locomotor activity was recorded on days 1, 21 and 28 using an actophotometer (INCO, Ambala, India) for a period of 10 min and expressed as counts per 10 min (Bansal et al. 2017).

### Rotarod test

Rotarod (Roxley Scientific Instruments, Ambala, India) apparatus was used to assess motor impairment in rats on days 1 and 21. For habituation, the rats were placed on constantly rotating rod (10 rpm) for 3 min. To determine motor coordination, each animal was placed on rod whose rotations gradually increased from 6 to 40 rpm over 5 min and latency to fall off (s) from rotating rod was noted.

**Fig. 1** Drug treatment schedule and experimental protocol



## Morris water maze test

Spatial navigation memory of rodents was assessed by using the Morris water maze (MWM) test in the place-condition paradigm which involves learning using allocentric and egocentric cues to escape on a submerged platform placed in a fixed location with the start position of each animal randomised with each trial (Morris 1984). A black-coloured metallic (iron) circular tank (diameter 200 cm, height 60 cm) was filled to a depth of 30 cm with water (temperature  $25 \pm 1$  °C), and two threads were fixed at the right angle to each other on the rim of the pool to divide the tank into four equal quadrants. A clockwise nomenclature was assigned to quadrants, viz. north (N), east (E), south (S) and west (W). The standard procedure was adopted having three phases. On day 21, each rat was familiarised with MWM by allowing maze exploration for 120 s without platform. During acquisition phase, a black-painted metal (iron) platform (area  $11 \text{ cm}^2$ , search area/target ratio of 314:1) was submerged 2 cm below the surface of water in the centre of target quadrant (W) of this tank. The platform was camouflaged by making the water opaque. In the place-condition paradigm, submerged platform was kept in a fixed location (W) throughout the training session with the start position of each animal randomised with each trial. The rat was smoothly released in the water with head facing the wall of the tank and allowed 120 s to locate submerged platform. The start location of each animal was randomised, viz. from N to W on day 22, from E to N on day 23, from S to E on day 24, from W to S on day 25 and from N to W on day 26 for each trial. Each rat received four training trials consecutively per day with an inter-trial gap of 30 s on the platform. The animal unable to locate the hidden platform within 120 s was guided gently onto the platform. The time taken by each rat to locate the hidden platform denotes mean escape latency (MEL). After 24 h of the last acquisition trial, retention of memory of each rat was determined in a probe trial. The platform was removed, each rat was placed  $180^\circ$  from the original platform position to navigate the tank for 60 s to eliminate thigmotaxis (Vorhees and Williams 2006) and the mean time spent in all four quadrants was noted. The reference memory is denoted by the percentage of mean time spent by the animal in target quadrant [TSTQ (%)] searching for the camouflaged platform. Twenty-four hours after the probe trial, a visible platform probe trial was performed to assess the visuospatial and sensorimotor performance of rats, with platform remaining at the same position but protruding 2 cm above the water level and covered by aluminum foil (Moosavi et al. 2014). The distal visual cues and position of experimenter remained the same during the whole study.

## Elevated plus maze test

The elevated plus maze (EPM) consisted of a wooden apparatus having a square central platform (area  $100 \text{ cm}^2$ ) connected to two open arms ( $50 \text{ cm} \times 10 \text{ cm}$ ) and two laterally covered arms with open roof ( $50 \text{ cm} \times 40 \text{ cm} \times 10 \text{ cm}$ ), placed 60 cm above the floor. The duration of entry of the rat from the open arm into one of the covered arms (transfer latency) with its entire four paws denoted memory of the animal. On day 27, each rat was placed at the distal most end of an open arm with head opposite to the central platform and allowed to explore the maze for 90 s. The animal which failed to passage into a closed arm within 90 s was gently guided in one of the covered arms. The rat was further given an exploration time of 20 s and then returned to its home cage. The memory of this EPM learning was evaluated 24 h after the last trial (Bansal et al. 2017).

## Whole brain homogenate preparation

For biochemical estimations ( $n = 5$ ), the rats were sacrificed by decapitation under light diethyl ether anaesthesia on day 28. The whole brain was dissected out and rinsed with ice-cold sterile normal saline (0.9 g/l sodium chloride) to eliminate the extraneous tissue residues and blood. Brain tissue homogenate (10% w/v) was prepared in 50 mM sodium potassium phosphate buffer (1% v/v Triton X-100, pH 7.4) at 4 °C and centrifuged at  $15 \times 10^3$  rpm for 20 min (4 °C) in high-speed refrigerated centrifuge (CPR-30 Remi Compufuge, India), and the supernatant was separated from the sediment for estimation of acetylcholinesterase (AChE), reduced glutathione (GSH), superoxide dismutase (SOD), catalase (CAT), nitrite and lactate dehydrogenase (LDH).

## Estimation of lipid peroxidation in the rat brain

Measurement of thiobarbituric acid-reactive substances (TBARS) is a reliable index of lipid peroxidation (pink-coloured malondialdehyde (MDA)-thiobarbituric acid (TBA)<sub>2</sub> adducts) and was measured by the method of Ohkawa et al. (1979). The 4 ml assay mixture consisted of 0.1 ml homogenate, 0.2 ml of 8.1% sodium dodecyl sulphate, 1.5 ml of 20% glacial acetic acid (pH 3.5), 1.5 ml of 0.8% TBA and 0.7 ml distilled water. Tubes were mixed, heated at 95 °C for 1 h on a water bath, cooled under tap water, vigorously mixed with 5 ml mixture of *n*-butanol and pyridine (15:1) and centrifuged at 4000 rpm for 10 min. The absorbance of upper 2 ml organic layer (*n*-butanol phase) was measured at a wavelength of  $\lambda_{\text{max}} = 532 \text{ nm}$  using a spectrophotometer (Shimadzu UV-1700, Pharmaspec). The amount of MDA formed or TBARS was calculated by using the molar extinction coefficient of chromophore  $1.56 \times 10^5 \text{ M}^{-1} \text{ cm}^{-1}$  and expressed as nanomoles/milligram of protein.

### Estimation of GSH in the rat brain

GSH was estimated according to the method of Ellman (1959). The 1-ml supernatant was precipitated with 1 ml of 4% sulphosalicylic acid, cold digested for 1 h at 4 °C and, after 5 min, centrifuged at 2000 rpm for 10 min at 4 °C. To 0.1 ml of the supernatant obtained, 2.7 ml of 0.3 M phosphate buffer (pH 8) and 0.2 ml of DTNB (0.1 mM, pH 8) were added. The absorbance was measured at  $\lambda_{\max} = 412$  nm using a spectrophotometer (Shimadzu UV-1700, Pharmaspec), and the amount of GSH (micromoles of GSH/milligram of protein) was calculated using the molar extinction coefficient  $1.36 \times 10^4 \text{ M}^{-1} \text{ cm}^{-1}$  of the chromophore.

### Determination of SOD activity in the rat brain

SOD (EC 1.15.1.1) activity was determined according to the method of Winterbourn et al. (1975) with slight modification. The reaction mixture contains 0.05 ml of the supernatant, 0.2 ml of 0.1 M EDTA (containing 0.0015% or 0.3 mM NaCN), 0.1 ml of 1.5 mM nitroblue tetrazolium (NBT), 0.05 ml of riboflavin (0.12 mM) and phosphate buffer (67 mM, pH 7.8) q.s. to make up the total volume of 3 ml. All the tubes were illuminated uniformly for 15 min under a 60 W Philips fluorescent bulb, and absorbance was measured at the  $\lambda_{\max} = 560$  nm wavelength for 5 min at 30-s intervals. The amount of NBT reduced was determined by the change in absorbance, based on the molar extinction coefficient of  $15,000 \text{ M}^{-1} \text{ cm}^{-1}$  for formazan, and the results were expressed as micromoles of NBT reduced/minute/milligram of protein.

### Determination of CAT activity in the brain of rats

CAT (EC 1.11.1.6) activity was assessed following the method of Claiborne (1985). The assay mixture consisted of 1.95 ml phosphate buffer (0.05 M, pH 7), 1 ml hydrogen peroxide (0.02 M, prepared in 0.05 M phosphate buffer) and 0.05 ml of the supernatant (10%) in a final volume of 3 ml. Decomposition of  $\text{H}_2\text{O}_2$  by catalase parallels with a decrease in absorbance at 240 nm. Change in absorbance for 3 min at 30-s intervals was recorded using a spectrophotometer. Enzymatic activity was calculated using the molar extinction coefficient of  $43.6 \text{ M}^{-1} \text{ cm}^{-1}$  at  $\lambda_{\max} = 240$  nm and expressed as micromoles of  $\text{H}_2\text{O}_2$  decomposed/minute/milligram of protein.

### Measurement of AChE activity in the brain of rats

The activity of acetylcholinesterase (EC 3.1.1.7) was assayed by the method of Ellman et al. (1961). Briefly, the reaction mixture consisted of 0.05 ml of the supernatant, 3 ml of phosphate buffer (100 mM, pH 8), 0.1 ml of 10 mM 5,5'-dithiobis-(2-nitrobenzoic acid) and 0.1 ml of acetylthiocholine

iodide (0.075 M; AThCh). AChE activity is expressed in micromoles of acetylthiocholine iodide hydrolysed/minute/milligram of protein ( $\epsilon = 1.36 \times 10^4 \text{ M}^{-1} \text{ cm}^{-1}$ ,  $\lambda_{\max} = 412$  nm).

### Determination of LDH in the rat brain

The lactate dehydrogenase (EC 1.1.1.27) activity was assayed by the method of Horecker and Kornberg (1948). The total reaction mixture (3 ml) contained 1 ml of 0.2 M Tris-HCl buffer (pH 7.4), 0.15 ml of 0.1 M KCl, 0.15 ml of 50 mM sodium pyruvate, 0.20 ml of 2.4 mM NADH and 1.5 ml of the supernatant. A decrease in extinction ( $6220 \text{ M}^{-1} \text{ cm}^{-1}$ ) at  $\lambda_{\max} = 340$  nm for 2 min at 25 °C was measured. The result was expressed in LDH activity in micromoles/minute/milligram of protein.

### Measurement of nitrite content in the rat brain

Total brain nitrite was assessed by the method of Sastry et al. (2002). Briefly, a mixture of 0.1 ml of the supernatant, 0.4 ml of carbonate buffer (pH 9) and 150 mg Cu-Cd alloy was incubated at room temperature for 1 h. The samples were allowed to stand for 10 min and then centrifuged at 4000 rpm for 10 min. A measure of 0.5 ml of the Griess reagent (1:1 solution of 1% sulphanilamide in 3 M HCl and 0.1% *N*-1-naphthyl ethylenediamine dihydrochloride in water) was added to 0.1 ml of the supernatant and mixture was incubated for 10 min at room temperature in the dark. Absorbance of deep purple-coloured azo compound was measured at  $\lambda_{\max} = 548$  nm wavelength. Standard curve of sodium nitrite (10–100  $\mu\text{M}$ ) was plotted to calculate the concentration of the test sample of nitrite (*n* micromole/mg of protein).

### Enzyme-linked immunosorbent assay

The rat brain eNOS (KINESISDx, California) and TNF- $\alpha$  (Krishgen, Mumbai) levels were determined by double-antibody sandwich enzyme-linked immunosorbent assay (ELISA) as per instructions provided in kits. The brain homogenate was centrifuged at 2500 rpm for 20 min, and the supernatant was used for ELISA procedures. The sample was added to rat monoclonal antibody-precoated wells (96 wells), treated with secondary antibodies labeled with biotin followed by streptavidin-horseradish peroxidase and incubated at 37 °C for 1 h after covering the plate. Afterwards, treatment with chromogenic solutions A and B or TMB substrate produced a bluish colour, a stop solution was added to stop the reaction and absorbance was noted at  $\lambda_{\max} = 450$  nm in an ELISA microplate reader (iMark, Bio-Rad) within 15 min of stopping reaction. The concentration of eNOS (ng/ml) and TNF- $\alpha$  (pg/ml) in the unknown sample was calculated from the standard curve.

## Estimation of total protein in the rat brain

The total protein of isolated brain tissue was determined by the method developed by Lowry et al. (1951). The reaction mixture consisted of 0.25 ml of the supernatant, 0.75 ml phosphate buffer, 5 ml of Lowry's reagent and 0.5 ml of the Folin-Ciocalteu reagent (1 N). After incubation, the protein content was determined spectrophotometrically at  $\lambda_{\max} = 650$  nm with a standard curve (0.25–2.50 mg/ml of bovine serum albumin).

## Histopathology of the rat brain

The rats ( $n = 1$ ) were deeply anaesthetised with chloral hydrate (400 mg/kg, i.p.) and transcardially perfused with 10% neutral buffered formalin (NBF) solution (10%). The head was decapitated; the brain was removed and fixed in 10% NBF (0.05% sodium azide, pH 7) in a 10:1 ratio of fixative to tissue for 6 days at 4 °C. Afterwards, the brain was stored in 70% ethanol at 4 °C until sectioning. Sections (5  $\mu$ m) were trimmed out by microtome and stained with haematoxylin and eosin (H&E). Slides were then cover slipped with permanent mounting medium (synthetic resin DPX) and examined in light microscopy at  $\times 100$  magnifications for pyknotic nuclei.

## Statistical analysis

One-way ANOVA followed by Tukey's post hoc test and two-way ANOVA followed by the Bonferroni post hoc test were utilised to interpret inter-group variation using software GraphPad Prism5 (GraphPad Software, Inc., USA). All the values are denoted as mean  $\pm$  SEM, and statistical significance was achieved at  $p < 0.05$ .

## Results

### Locomotor activity of rats was unaffected by different treatments

The mean locomotor activity scores of days 1, 21 and 28 exhibited no significant difference between different groups (Fig. 2).

### Motor coordination of rats was not altered by various treatments

In the present study, the mean fall-off latency (s) from the rotating rod did not differ significantly among rats of all the groups as determined on days 1 and 21 (Fig. 3).

### Prevention of learning and memory impairment in STZ-ICV-treated rats by EGA is attenuated by wortmannin and L-NAME in the MWM paradigm

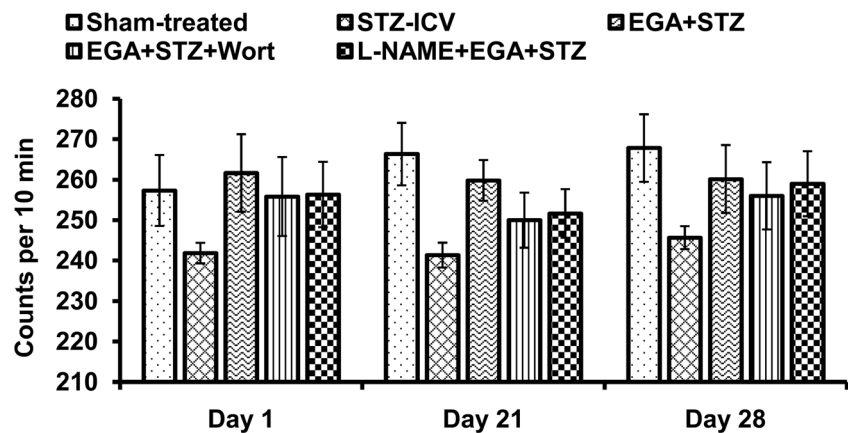
Consistent with previous findings, there was no significant difference in MEL among all the groups on day 22 of acquisition trials in MWM, but major differences emerged out on day 23. The rats administered with STZ-ICV alone exhibited poor spatial learning evident by significantly ( $p < 0.001$ ) higher MEL with respect to rats of the sham-treated group. Oral administration of EGA (35 mg/kg) attenuated ( $p < 0.001$ ) the STZ-ICV-induced increase of MEL when compared to the STZ-ICV alone group and thereby manifested improvement in learning of rats. The wortmannin (PI3-kinase inhibitor) group portrayed considerable rise ( $p < 0.001$ ) in MEL in comparison to the EGA+STZ group; however, the MEL was lower ( $p < 0.001$ ) in the STZ-ICV group. The L-NAME (eNOS inhibitor) group exhibited enhanced ( $p < 0.001$ ) MEL in comparison to the EGA+STZ group but exhibited a considerable decline ( $p < 0.001$ ) of MEL with respect to the wortmannin group (Fig. 4a).

The probe trial was conducted on day 27 to assess the memory of rats. The STZ-ICV alone group exhibited a profound decrease ( $p < 0.001$ ) in the percentage of time spent in the target quadrant [TSTQ (%)] with respect to rats of the sham-treated group and thereby denoted cognitive dysfunction. The EGA+STZ group spent significantly ( $p < 0.001$ ) more time in the target quadrant when compared with the STZ-ICV alone group depicting attenuation of memory dysfunction. A decline ( $p < 0.001$ ) of TSTQ (%) in the wortmannin group was noted in comparison to the EGA+STZ group. However, the wortmannin group revealed a higher ( $p < 0.05$ ) TSTQ (%) than the STZ-ICV alone group. The L-NAME group displayed downfall of TSTQ (%) ( $p < 0.001$ ) in comparison to the EGA+STZ group, though improved TSTQ (%) with respect to the wortmannin group ( $p < 0.05$ ) (Fig. 4b). The MWM results disclosed that in the STZ-ICV model, wortmannin (PI3-kinase inhibitor) or L-NAME (NOS inhibitor) treatments impeded the memory-enhancing activity of EGA. No significant difference between MEL of different groups was observed during the visible platform trial which pointed intact sensorimotor function and visuospatial acuity in rats (Fig. 4c).

### Wortmannin and L-NAME preclude EGA-induced memory enhancement of STZ-ICV-treated rats in the EPM task

None of the groups depicted significant variation in mean transfer latency (TL) on day 27 during the acquisition trial of the EPM task. In the retrieval trial on day 28, an increase ( $p < 0.001$ ) in mean TL was observed in the STZ-ICV group when compared to the sham-treated group which signified

**Fig. 2** Mean ambulatory scores in the actophotometer showed no significant variation. Two-way ANOVA followed by the Bonferroni post hoc test was applied. Values are expressed as mean  $\pm$  SEM ( $n = 6$ )



loss of memory. The EGA+STZ group showed a decline ( $p < 0.001$ ) of TL in comparison to the STZ-ICV group. The Wortmannin group displayed enhanced ( $p < 0.001$ ) TL in comparison to the EGA+STZ group, but TL was lower than that in the STZ-ICV alone group. The L-NAME group exhibited a considerable delay ( $p < 0.001$ ) of TL in the closed arm of EPM with respect to the EGA+STZ group but showed improvement in TL ( $p < 0.05$ ) when compared to the wortmannin group (Fig. 5).

#### Wortmannin and L-NAME enhance STZ-ICV-induced brain lipid peroxidation in EGA-treated rats

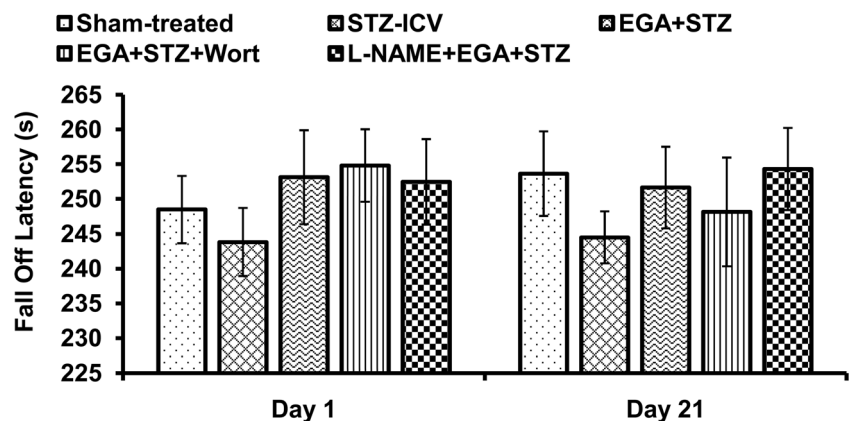
Measurement of TBARS quantifies the lipid peroxidation product MDA, an established biomarker of oxidative stress. Central administration of STZ elevated the brain TBARS content ( $p < 0.001$ ) in comparison to sham-treated rats. Chronic EGA treatment arrested the STZ-ICV-induced surge in TBARS content ( $p < 0.001$ ) in the brain of rats as compared to rats that received STZ-ICV alone. ICV administration of wortmannin (PI3-kinase inhibitor) augmented ( $p < 0.001$ ) the TBARS content in the brain of EGA- and STZ-ICV-treated rats with respect to rats that received EGA and STZ-ICV only.

Administration of L-NAME (eNOS inhibitor) conspicuously raised the whole-brain TBARS level ( $p < 0.001$ ) in EGA- and STZ-ICV-treated rats with respect to rats that received EGA and STZ-ICV only. However, the L-NAME group showed significantly lower brain TBARS content ( $p < 0.01$ ) than the wortmannin group (Fig. 6a). These results suggested the rise of oxidative stress in response to inhibition of eNOS activity by wortmannin and L-NAME in EGA- and STZ-ICV-treated rats.

#### Wortmannin and L-NAME reduce GSH content in the brain of EGA- and STZ-ICV-treated rats

Centrally administered STZ subsided the whole-brain GSH level ( $p < 0.001$ ) in comparison to sham treatment. Chronic treatment with EGA prohibited the STZ-ICV-triggered decrease in brain GSH level ( $p < 0.001$ ) in rats with respect to rats that received STZ-ICV alone. The wortmannin group manifested lower GSH level ( $p < 0.001$ ) with respect to the EGA+STZ group. Administration of L-NAME (eNOS inhibitor) for 4 weeks daily diminished the whole-brain GSH content ( $p < 0.001$ ) in EGA- and STZ-ICV-treated rats with respect to rats that received EGA and STZ-ICV only. However,

**Fig. 3** Different groups have no significant variation in latency to fall off (s) determined by utilising a rotarod apparatus. One-way ANOVA followed by Tukey's post hoc test was applied. Values are denoted as mean  $\pm$  SEM ( $n = 6$ )



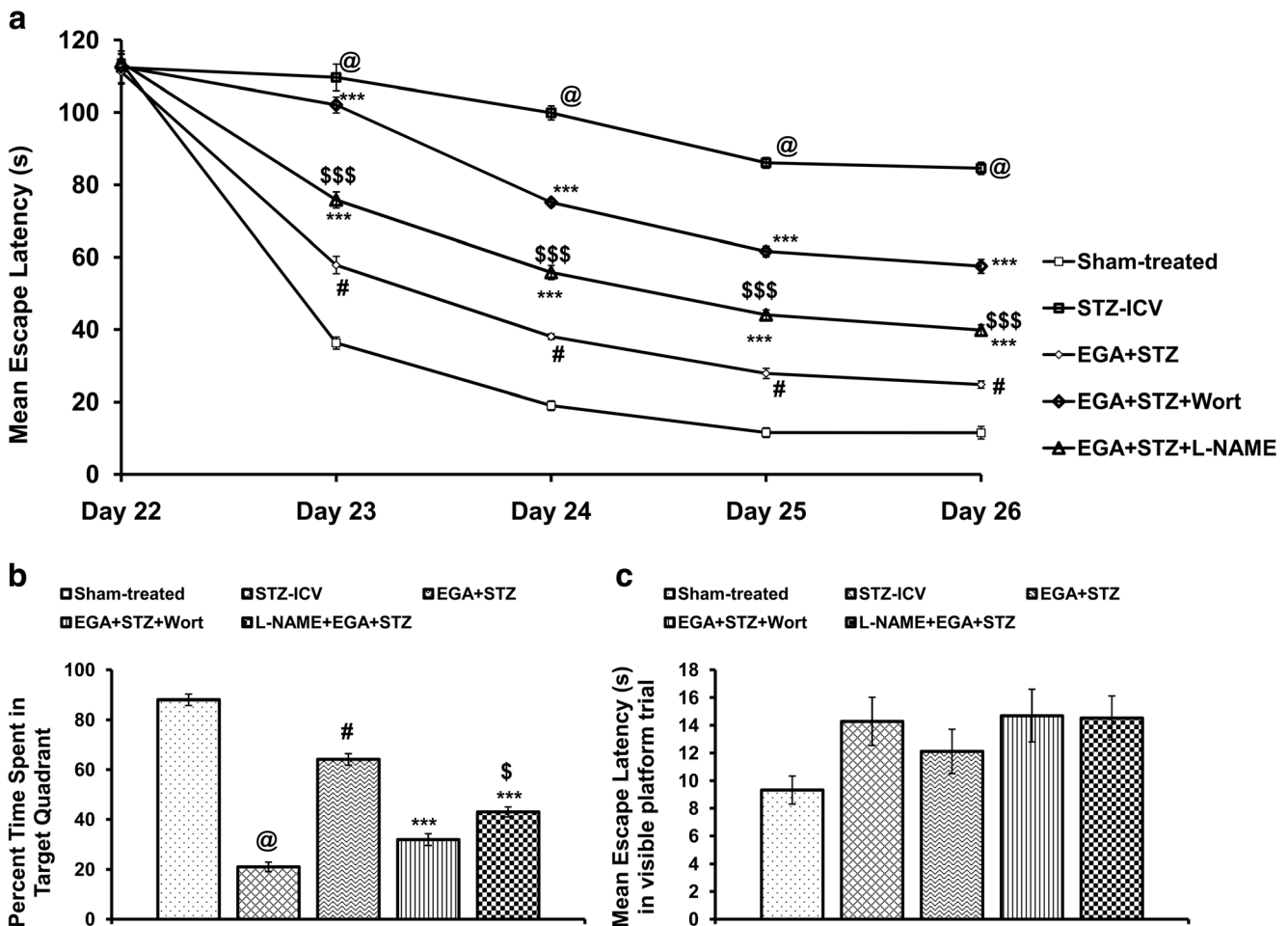


**Fig. 4** Wortmannin (5  $\mu\text{g}/\text{rat}$ ) and L-NAME (20  $\text{mg}/\text{kg}$ ) treatments attenuate EGA (35  $\text{mg}/\text{kg}$ )-induced learning and memory enhancement in STZ-ICV-treated rats. Statistical comparison of **a** mean escape latency (MEL) during the 5-day acquisition trials in MWM (two-way ANOVA followed by the Bonferroni post hoc test was applied). **b** Percentage of time spent in the target quadrant [TSTQ(%)] during the probe trial in MWM (one-way ANOVA followed by Tukey's post hoc test was

applied). **c** Mean escape latency during the visible platform trial to assess the sensorimotor and visuospatial functions of rats in MWM (one-way ANOVA followed by Tukey's post hoc test was applied). Values are expressed as mean  $\pm$  SEM ( $n=6$ ). Significance at  $^{\textcircled{a}}$   $p < 0.001$  vs. the sham-treated group;  $^{\#}$   $p < 0.001$  vs. the STZ-ICV group;  $^{***}$   $p < 0.001$  vs. the EGA+STZ group;  $^{\textcircled{S}}$   $p < 0.05$  and  $^{\textcircled{SSS}}$   $p < 0.001$  vs. the EGA+STZ+Wort group

the L-NAME group showed a significant elevation in GSH level ( $p < 0.01$ ) than the wortmannin group (Fig. 6b).

### Wortmannin and L-NAME reduce SOD activity in the brain of EGA- and STZ-ICV-treated rats

STZ-ICV treatment diminished the whole-brain SOD activity ( $p < 0.001$ ) in comparison to sham treatment. Administration of EGA for 4 weeks daily attenuated the STZ-ICV-induced reduction of brain SOD activity ( $p < 0.001$ ) in comparison to STZ-ICV alone treatment. ICV administration of wortmannin (PI3-kinase inhibitor) to EGA- and STZ-ICV-treated rats lowered the SOD activity ( $p < 0.001$ ) in comparison to rats that received EGA and STZ-ICV only. Chronic treatment with L-NAME (eNOS inhibitor) decreased the SOD activity ( $p < 0.05$ ) in the brain of EGA- and STZ-ICV-treated rats with

respect to rats that received EGA and STZ-ICV only. However, the L-NAME group showed a significant increase in SOD activity ( $p < 0.001$ ) than the wortmannin group (Fig. 6c).

### Wortmannin and L-NAME diminish the CAT activity in the brain of EGA- and STZ-ICV-treated rats

ICV administration of STZ abated the brain CAT activity ( $p < 0.001$ ) in comparison to sham treatment. Orally administered EGA arrested the dwindling CAT activity ( $p < 0.001$ ) in the brain of STZ-ICV-treated rats when compared to rats treated with STZ-ICV alone. Centrally administered wortmannin (PI3-kinase inhibitor) impeded the restoration of brain CAT activity ( $p < 0.001$ ) by EGA in STZ-ICV-treated rats in comparison to rats that received EGA and STZ-ICV only. Long-



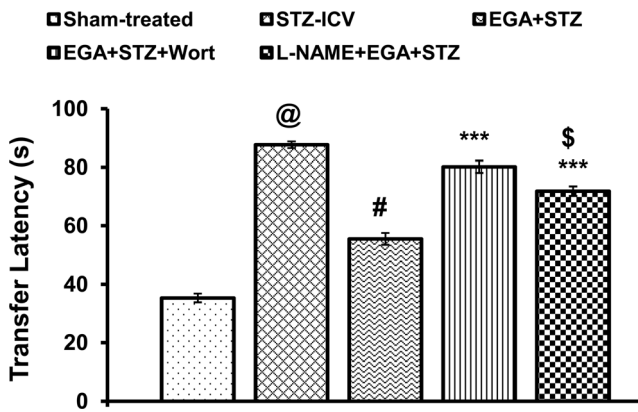


**Fig. 5** Wortmannin (5 µg/rat) and L-NAME (20 mg/kg) treatments impeded the prevention of STZ-ICV-triggered memory dysfunction by EGA (35 mg/kg). Statistical comparison of mean transfer latency (s) during the retrieval trial in EPM (one-way ANOVA followed by Tukey's post hoc test was applied). Values are expressed as mean ± SEM (n = 6). Significance at <sup>@</sup>p < 0.001 vs. the sham-treated group; <sup>#</sup>p < 0.001 vs. the STZ-ICV group; <sup>\*\*\*</sup>p < 0.001 vs. the EGA+STZ group; <sup>§</sup>p < 0.05 vs. the EGA+STZ+Wort group

term treatment with L-NAME diminished the CAT activity (p < 0.001) in the brain of EGA- and STZ-ICV-treated rats with respect to rats that received EGA and STZ-ICV only.

However, the L-NAME group showed a significant elevation in CAT activity (p < 0.01) than the wortmannin group (Fig. 6d).

### Wortmannin and L-NAME attenuate brain AChE inhibitory activity of EGA in STZ-ICV-treated rats

The STZ-ICV group showed a significant increase (p < 0.001) in whole-brain AChE activity in comparison to the sham-treated group. EGA attenuated (p < 0.001) the STZ-ICV-induced rise of AChE activity in the brain of rats as compared to rats that received STZ-ICV alone. L-NAME and wortmannin groups exhibited a significant increase in AChE activity (p < 0.01 and p < 0.001, respectively) with respect to the EGA+STZ group (Fig. 7a). However, the brain AChE activity of the L-NAME group was significantly (p < 0.05) lower than that of the wortmannin group. These results showed that suppression of NO biosynthesis by L-NAME (competitive NOS inhibitor) or wortmannin (PI3-kinase-eNOS blocker) impeded the AChE inhibitory activity of EGA and thereby attenuated cholinergic function in the brain of rats.

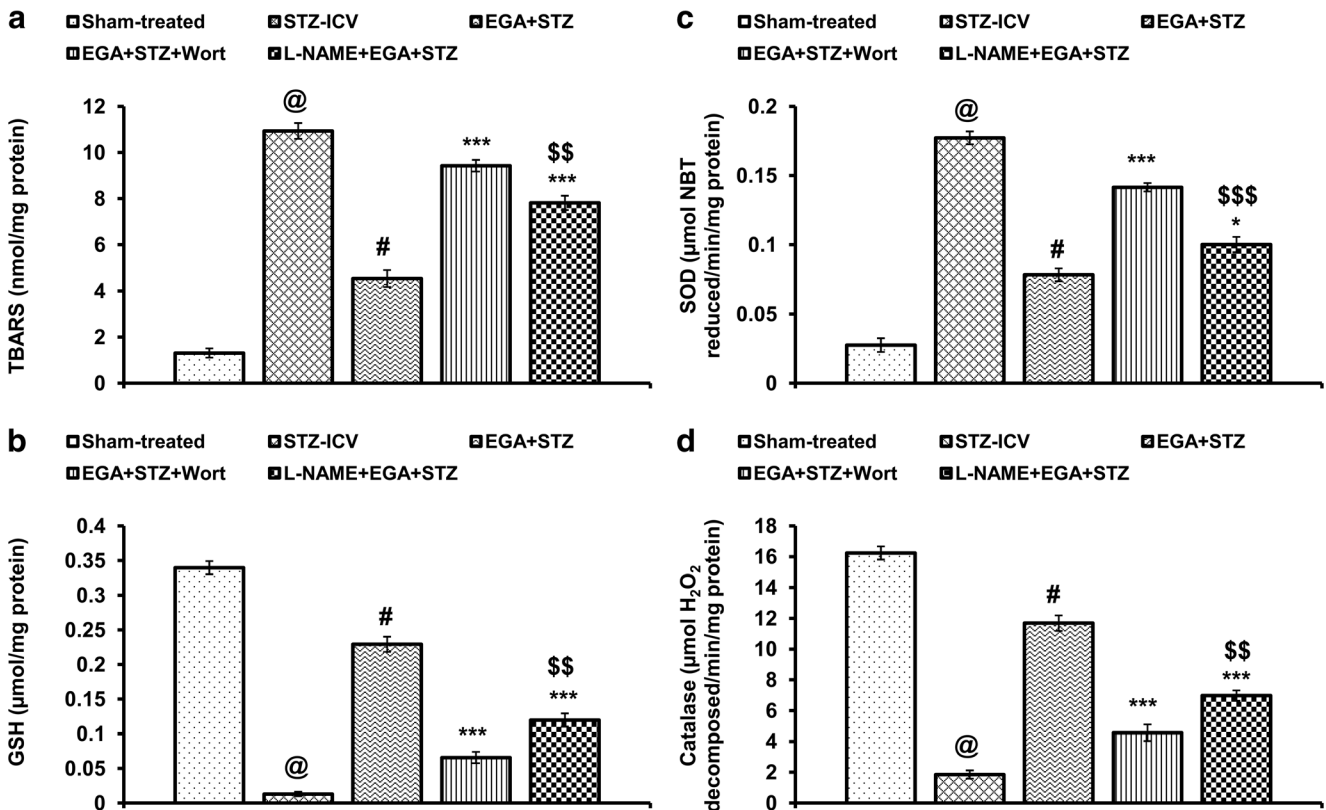


**Fig. 6** Modulation of markers of oxidative stress by wortmannin (5 µg/rat) and L-NAME (20 mg/kg) in the brain of EGA- (35 mg/kg) and STZ-ICV-treated rats. Statistical comparison of the brain **a** thiobarbituric acid reactive substances (TBARS) content, **b** reduced glutathione (GSH) level, **c** superoxide dismutase (SOD) activity and **d** catalase (CAT) activity in

different groups (one-way ANOVA followed by Tukey's post hoc test was applied). Values are expressed as mean ± SEM (n = 5). Significance at <sup>@</sup>p < 0.001 vs. the sham-treated group; <sup>#</sup>p < 0.001 vs. the STZ-ICV group; <sup>\*</sup>p < 0.05 and <sup>\*\*\*</sup>p < 0.001 vs. the EGA+STZ group; <sup>§§</sup>p < 0.01 and <sup>§§§</sup>p < 0.001 vs. the EGA+STZ+Wort group

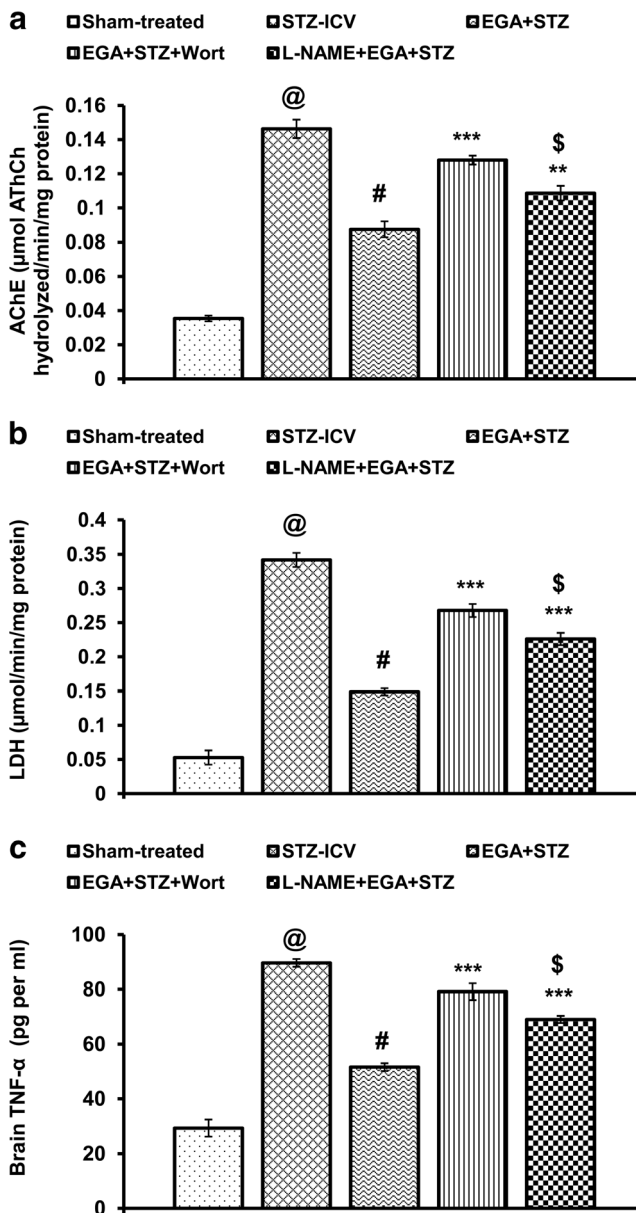


**Fig. 7** Modulation of brain acetylcholinesterase (AChE), lactate dehydrogenase (LDH) and TNF- $\alpha$  by wortmannin (5  $\mu$ g/rat) and L-NAME (20 mg/kg) in EGA- (35 mg/kg) and STZ-ICV-treated rats. Statistical analysis of the brain **a** AChE activity, **b** LDH activity and **c** TNF- $\alpha$  content in different groups (one-way ANOVA followed by Tukey's post hoc test was applied). Values are expressed as mean  $\pm$  SEM ( $n = 5$ ). Significance at <sup>@</sup> $p < 0.001$  vs. the sham-treated group; <sup>#</sup> $p < 0.001$  vs. the STZ-ICV group; <sup>\*\*</sup> $p < 0.01$  and <sup>\*\*\*</sup> $p < 0.001$  vs. the EGA+STZ group; <sup>§</sup> $p < 0.05$  vs. the EGA+STZ+Wort group

### Wortmannin and L-NAME enhance STZ-ICV-induced brain LDH activity in EGA-treated rats

An increase in LDH activity in the brain manifests disruption of neuron integrity and cell death. The rats of the STZ-ICV group exhibited an exorbitant rise ( $p < 0.001$ ) in brain LDH activity in comparison to rats of the sham-treated group. Administration of EGA subsided ( $p < 0.001$ ) the STZ-ICV-

triggered rise in the brain LDH activity as compared to STZ-ICV alone treatment. The L-NAME and wortmannin groups displayed high ( $p < 0.001$ ) brain LDH activity with respect to the EGA+STZ group. However, the brain LDH activity of the L-NAME group was significantly ( $p < 0.05$ ) lower than that of the wortmannin group (Fig. 7b). These findings indicated prevention of STZ-ICV-triggered neurodegeneration by EGA through PI3-kinase pathway.

### Wortmannin and L-NAME enhance STZ-ICV-induced increase of brain TNF- $\alpha$ level in EGA-treated rats

A significant ( $p < 0.001$ ) rise in brain TNF- $\alpha$  level was observed in STZ-ICV group rats as compared to rats of the sham-treated group. Chronic treatment with EGA attenuated ( $p < 0.001$ ) the brain TNF- $\alpha$  levels of STZ-ICV-administered rats with respect to rats that received STZ-ICV alone. L-NAME or wortmannin treatment abolished ( $p < 0.001$ ) the subsidence of brain TNF- $\alpha$  by EGA in separate groups of STZ-ICV-treated rats when compared to rats administered with EGA and STZ-ICV only. However, the brain of the L-NAME-treated group exhibited considerably low ( $p < 0.05$ ) TNF- $\alpha$  levels in comparison to that of the wortmannin-treated group (Fig. 7c). These findings suggested enhancement in neuroinflammation in response to inhibition of PI3-kinase and eNOS activity in the brain of rats. However, EGA was able to exert an anti-inflammatory effect by rescuing STZ-ICV-triggered downregulation of brain PI3-kinase pathway.

### Wortmannin and L-NAME potentiate the reduction of total brain nitrite content by EGA in STZ-ICV-treated rats

The STZ-ICV administration significantly ( $p < 0.001$ ) increased the brain nitrite content in comparison to sham treatment. The EGA+STZ group depicted low ( $p < 0.001$ ) brain nitrite content as compared to the STZ-ICV group. L-NAME (NOS inhibitor) or wortmannin (PI3-kinase inhibitor) treatment potentiated ( $p < 0.001$  and  $p < 0.01$ , respectively) the EGA-induced reduction of the brain nitrite content in separate groups of STZ-ICV-treated rats. The brain nitrite level of the wortmannin group was significantly ( $p < 0.05$ ) higher than of the L-NAME group. These results suggested implication of the compensatory role of NOS isoforms (Fig. 8a).

### Wortmannin and L-NAME alter the effect of EGA on brain endothelial NOS in STZ-ICV-treated rats

Administration of STZ-ICV alone diminished ( $p < 0.001$ ) the brain eNOS levels with respect to sham treatment, implying disruption of PI3-kinase activity in the brain of rats. Chronic treatment with EGA prevented ( $p < 0.001$ ) the STZ-ICV-

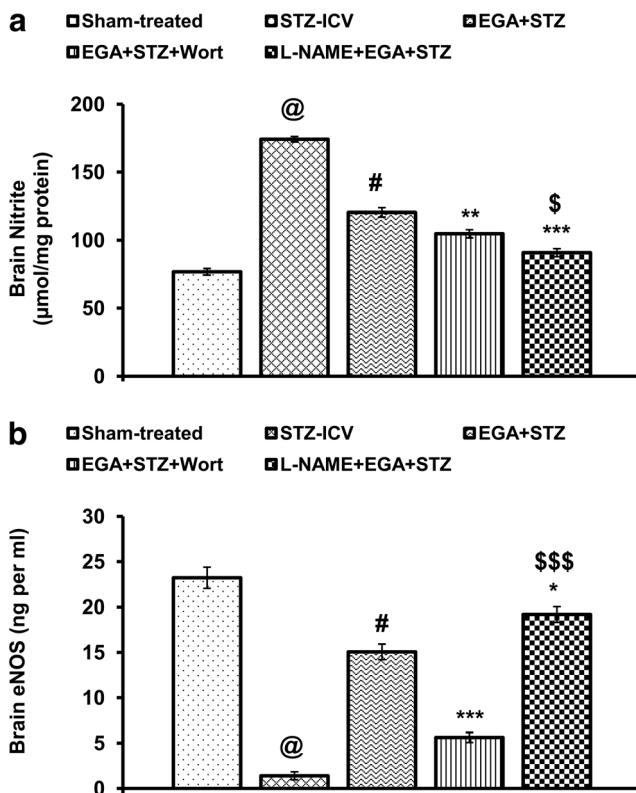


**Fig. 8** Modulation of the brain nitrite content and endothelial nitric oxide (eNOS) activity by wortmannin (5 µg/rat) and L-NAME (20 mg/kg) in EGA- (35 mg/kg) and STZ-ICV-treated rats. Statistical analysis of the brain **a** total nitrite content and **b** eNOS level in different groups (one-way ANOVA followed by Tukey's post hoc test was applied). Values are expressed as mean ± SEM ( $n = 5$ ). Significance at <sup>@</sup> $p < 0.001$  vs. the sham-treated group; <sup>#</sup> $p < 0.001$  vs. the STZ-ICV group; <sup>\*</sup> $p < 0.05$ , <sup>\*\*</sup> $p < 0.01$  and <sup>\*\*\*</sup> $p < 0.001$  vs. the EGA+STZ group; <sup>\$\$\$</sup> $p < 0.001$  vs. the EGA+STZ+Wort group

triggered decrease in brain eNOS function when compared with STZ-ICV alone treatment. The L-NAME (competitive eNOS inhibitor) group exhibited rise in brain eNOS content (not activity) with respect to EGA+STZ ( $p < 0.05$ ) and wortmannin ( $p < 0.001$ ) groups. Upregulation eNOS expression in the brain of EGA- and STZ-ICV-treated rats through suppression of nitric oxide transmission by L-NAME suggested that eNOS activity is under feedback control of NO. Inhibition of PI3-kinase activity by wortmannin impeded ( $p < 0.001$ ) the EGA-induced rise in eNOS expression and the activity in the brain of STZ-ICV-treated rats with respect to rats that received EGA and STZ-ICV only (Fig. 8b). These results imply that eNOS is under control of PI3-kinase at transcription level.

### Histology of the rat brain

The brain histology of sham group rats showed intact neurons. STZ-ICV injection instigated profound neurodegeneration in the cortical region of the rat brain. Chronic administration of EGA (35 mg/kg; p.o.) for 4 weeks daily prevented the brain of

rats from neurotoxicity of STZ-ICV treatment. L-NAME and wortmannin groups also showed conspicuous neurodegeneration (Fig. 9).

### Discussion

STZ is an *N*-methyl-*N*-nitrosourea-derived microbial product that simulates dementia akin to AD when administered centrally in dose ranges 1–3 mg/kg in rodents. STZ-triggered insulin resistance and reduction in cerebral blood flow are congruous with impairment of PI3-kinase and eNOS signalling (Agrawal et al. 2011; Rajasekar et al. 2017). Downfall of PI3-kinase-eNOS signalling in response to diabetogenic property of STZ conjures exaggeration of mitochondrial free radical generation and microglial pro-inflammatory cytokine release (Meng et al. 2017). PI3-kinase pathway plays a vital role in cellular respiration by facilitating insulin-mediated glucose metabolism. Correspondingly, aberration in PI3-kinase activity disrupts the mitochondrial aerobic respiration that accentuates ROS production (Zhao et al. 2017).

In the present study, ICV administration of STZ elevated the TBARS content and decreased the GSH levels and SOD and CAT activity in the brain of rats. TBARS, GSH, SOD and CAT constitute biomarkers of oxidative stress markedly altered very early in the AD affected brain. Surfeit of lipid peroxidation (TBARS) and depletion of brain antioxidant defense (GSH, SOD, CAT) ruin neuronal coherence and cognitive prowess (Sharma et al. 2010). Chronic EGA administration attenuated the brain lipid peroxidation (TBARS) and prevented waning of GSH, SOD and CAT activity in STZ-ICV-treated rats. These results are consistent with findings reported in earlier studies as the antioxidative property of EGA has been explored in a number of disorders such as cancer, colitis and diabetes (Landete 2011). Previous findings confirm that NO bestows antioxidant activity through interruption of free radical chain reaction and formation of biologically stable *S*-nitrosothiols with SH groups (e.g. *S*-nitrosoglutathione) (Paul and Ekambaram 2011). Commensurate with earlier reports, in the present study, suppression of eNOS activity by L-NAME (direct eNOS inhibitor) or wortmannin (PI3-kinase inhibitor) aggravated the lipid peroxidation (TBARS) and vanished the endogenous antioxidant guard (GSH, SOD, CAT) in the brain of EGA- and STZ-ICV-treated rats. However, the L-NAME group showed low TBARS level and superior GSH content and SOD and CAT activity as compared to the wortmannin group. These results demonstrated that competitive inhibition of eNOS activity by L-NAME or through interruption of PI3-kinase activity by wortmannin provided impetus to oxidative stress and decimated the antioxidant shield in the brain of EGA- and STZ-ICV-treated rats.

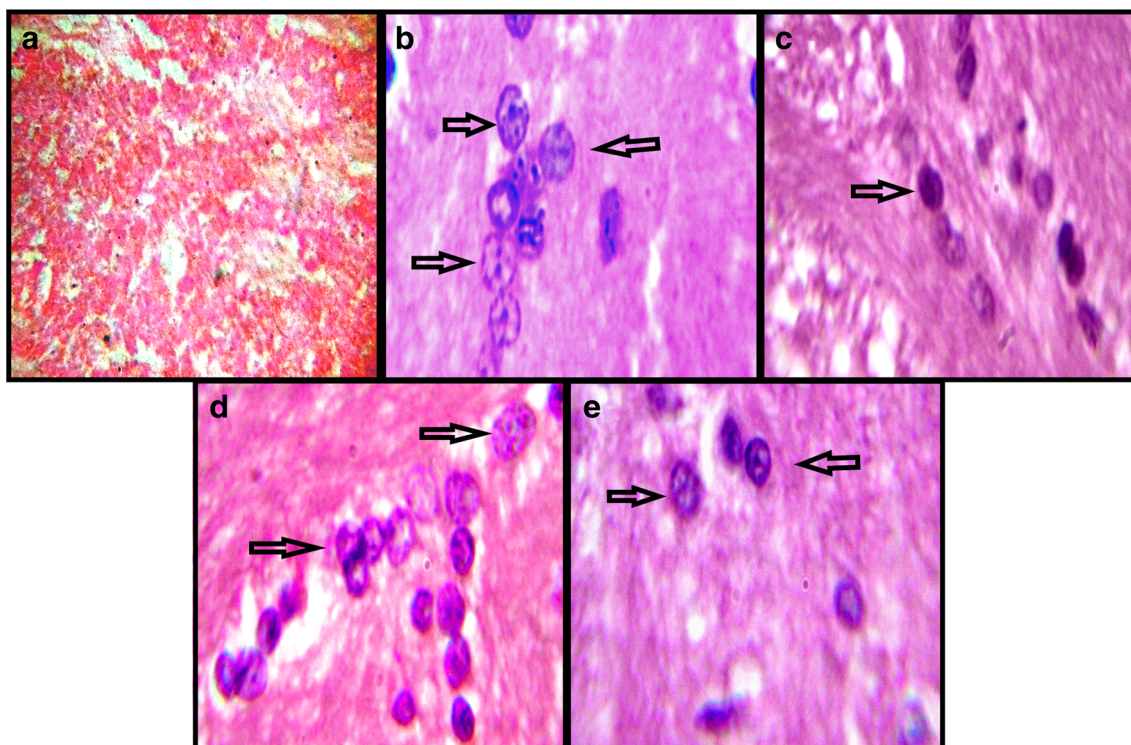


**Fig. 9** Histology of the rat ( $n = 1$ ) brain cortex (H&E,  $\times 100$ ; arrow mark indicates degenerated neurons). **a** Sham-treated group. **b** STZ-ICV group. **c** EGA+STZ group. **d** Wortmannin group (EGA+STZ+Wort). **e** L-NAME group (L-NAME+EGA+STZ)

TNF- $\alpha$  is a pro-inflammatory cytokine associated with numerous cellular responses such as excitotoxicity, inflammation, apoptosis and necrosis. Release of TNF- $\alpha$  by reactive microglia and astrocytes in response to immunogenic brain insult (e.g. TBI, A $\beta$  or STZ) are a characteristic feature of the AD affected brain (Calsolaro and Edison 2016). In the present study, administration of EGA for 4 weeks daily attenuated the STZ-ICV-triggered pathogenic release of TNF- $\alpha$  in the brain of rats. PI3-kinase dysfunction-originated A $\beta_{40-42}$  aggregates are known to exacerbate chronic inflammation in the brain by activating microglia through TLRs, RAGE and NODRs (Doens and Fernandez 2014). Competitive inhibition of eNOS and suppression of PI3-kinase-eNOS signalling by L-NAME and wortmannin respectively blocked the anti-inflammatory activity of EGA in the brain of STZ-ICV-treated rats. Earlier reports also substantiate the increase in brain TNF- $\alpha$  expression by inhibition of PI3-kinase activity by wortmannin or LY294002 and eNOS by L-NAME (Guha and Mackman 2002; Harry et al. 2001). However, wortmannin treatment raised the brain TNF- $\alpha$  level conspicuously in comparison to L-NAME treatment in EGA- and STZ-ICV-administered rats. Oxidative stress and inflammation compromise the neuron integrity quantified by measurement of brain LDH activity. LDH is a widely acclaimed biomarker of cell death. ICV administration of STZ induced profound neurodegeneration as indicated by high LDH activity determined in the brain of rats (Sharma et al. 2010). EGA

treatment attenuated the STZ-ICV-induced rise in brain LDH activity and concomitant neurodegeneration. Worsening of the free radical toxicity and inflammation amplified the LDH activity and subsequent brain tissue breakdown in the L-NAME group. Wortmannin (PI3-kinase inhibitor) treatment accelerated the brain LDH activity which suggested pro-survival activity of PI3-kinase pathway in EGA- and STZ-ICV-treated rats. These biochemical results were well supported by histopathological studies which showed neuron death. The wortmannin group exhibited higher LDH activity with respect to the L-NAME group. This study elucidates that the anti-inflammatory and pro-survival effects of EGA in the STZ-ICV model are mediated through PI3-kinase-eNOS signalling.

Neuronal and endothelial NOS-derived NO performs pleiotropic functions in the brain associated with synaptic plasticity and long-term potentiation. However, superfluous NO generation by inducible NOS (iNOS) may precipitate neurotoxicity through peroxynitrite, genotoxicity, PARP, inhibition of mitochondrial aerobic respiration and glutamate excitotoxicity (Murphy 1999). STZ is a nitrosourea derivative metabolised to NO in vivo, triggers iNOS activity (Rajasekar et al. 2017) and diminishes the expression and activity of eNOS through PI3-kinase dysfunction (Bedse et al. 2015). Analogous to previous studies, a surge of brain nitrite content in STZ-ICV-treated rats was noted. However, downfall in brain eNOS level in the STZ-ICV group indicated alteration

of the PI3-kinase pathway. Dysfunction of eNOS in stroke, experimentally induced brain ischemia and through specific eNOS inhibitors (e.g. L-N<sup>5</sup>-(1-iminoethyl) ornithine or diphenyleneiodonium chloride) has been associated with loss of neurotrophic factors (BDNF, NGF) and memory (Li et al. 2014; Provias and Jeynes 2008). EGA negated the STZ-ICV-induced outrageous rise of nitrite content and downregulation of eNOS level in the brain of rats. L-NAME and wortmannin treatments vigorously potentiated the decrease of brain nitrite content by EGA in STZ-ICV-treated rats. Chronic administration of L-NAME caused a profound decline in brain nitrite level as it is a relatively specific arginine-derived competitive eNOS inhibitor which binds with L-arginine binding site. In the STZ-ICV AD model, chronic administration of L-NAME elevated the brain eNOS level (not activity) in EGA-treated rats. Previous findings suggested that eNOS expression is a function of NO transmission and glucose metabolism (Mohan et al. 2012). ICV administration of wortmannin (PI3-kinase inhibitor) attenuated the rise of eNOS expression and activity by EGA in STZ-ICV-treated rats. In currently employed AD model, upregulation of PI3-kinase-regulated eNOS activity exhibited a vital role in the prevention of noxious effects of STZ-ICV by EGA.

Numerous CNS studies have shown that loss of the brain cholinergic activity deteriorates cognitive functions. Acetylcholine is involved in brain development, cerebral blood flow, sleep-wake cycle and memory (Ferreira-Vieira et al. 2016). In earlier studies, endogenous acetylcholine and anti-cholinesterase drugs (e.g. donepezil, rivastigmine) are shown to facilitate brain cholinergic activity through the PI3-kinase pathway (Resende and Adhikari 2009; Tyagi et al. 2010). Impairment in cellular glucose metabolism ruins brain acetylcholine status through acetylcholinesterase hyperactivity, energy deficit, thiamine depletion or degeneration of cholinergic neurons (Sharma et al. 2010). In this study, ICV administration of diabetogenic compound, STZ, caused profound enhancement in the AChE activity in the brain of rats. Administration of EGA lowered the AChE activity and thereby rescued a cholinergic decline in the brain of STZ-ICV-treated rats. L-NAME and wortmannin groups exhibited high brain AChE activity, implying a brain cholinergic deficit. In previous studies, a decrease in NO transmission is associated with impairment of brain cholinergic function (Prast et al. 1995). The wortmannin group showed profound brain cholinergic hypofunction in comparison to the L-NAME group. The present study corroborates that PI3-kinase-eNOS signalling is involved in cholinergic augmentation by EGA in the brain of STZ-ICV-treated rats.

The behavioral tests demonstrated that STZ-ICV treatment invoked oxidative stress, inflammation, cholinergic deficit and loss of eNOS activity-culminated profound cognitive decline in rats. Chronic administration of EGA lessened the neurotoxic influence of STZ-ICV

in the rat brain and subsequently augmented their memory functions. These results substantiate the therapeutic benefits of EGA as a nutraceutical in promotion of mental health. L-NAME treatment inhibited the eNOS activity and thereby accrued oxidative stress and inflammation and hampered the memory functions in the brain of EGA- and STZ-ICV-treated rats. ICV-administered wortmannin (PI3-kinase inhibitor) stymied the EGA activities and redemption of cognitive abilities in STZ-ICV-treated rats. However, the L-NAME group portrayed better memory in comparison to the wortmannin group. The visuospatial and sensorimotor abilities of rats determined during the visible platform trial remained intact in response to chronic L-NAME treatment. The locomotor activity and motor coordination of rats were unaffected by different treatments.

## Conclusions

In the presently employed STZ-ICV model of AD, suppression of the brain PI3-kinase-eNOS activity by wortmannin (PI3-kinase inhibitor) or direct competitive inhibition of eNOS by L-NAME impeded the brain cholinergic, antioxidative, anti-inflammatory, pro-survival and memory-enhancing functions of EGA in rats. However, brain eNOS expression (not activity) was enhanced by L-NAME and reduced by wortmannin in EGA- and STZ-ICV-treated rats. In behavioral studies, the wortmannin group showed profound loss of cognitive abilities in comparison to the L-NAME group. Hence, it is highly pertinent to conclude that EGA averted the STZ-ICV-induced loss of brain PI3-kinase-eNOS activity and thereby prevented the memory deficits in rats. The present study emphasises that EGA or EGA-fortified supplements are brain tonics having potent therapeutic potential in allaying neurodegenerative disorders such as AD.

**Acknowledgements** The authors are thankful to the management of ASBASJSM College of Pharmacy, Bela, for providing the necessary research facilities and IKG Punjab Technical University, Kapurthala.

**Authors' contribution** Prof. (Dr.) Nitin Bansal designed this study. Manish Kumar (PhD research scholar) conducted the research and analysed and interpreted the data. Both authors wrote the initial and final draft of the article.

**Funding information** This research was assisted by a grant from AICTE, New Delhi (India), under Research Promotion Scheme.

## Compliance with ethical standards

**Conflict of interest** The authors declare that they have no conflict of interest.

## References

- Agrawal R, Tyagi E, Shukla R, Nath C (2011) Insulin receptor signaling in rat hippocampus: a study in STZ (ICV) induced memory deficit model. *Eur Neuropsychopharmacol* 21:261–273. <https://doi.org/10.1016/j.euroneuro.2010.11.009>
- Austin SA, Santhanam AV, Hinton DJ, Choi DS, Katusic ZS (2013) Endothelial nitric oxide deficiency promotes Alzheimer's disease pathology. *J Neurochem* 127:691–700. <https://doi.org/10.1111/jnc.12334>
- Baki L, Shioi J, Wen P, Shao Z, Schwarzman A, Gama-Sosa M, Neve R, Robakis N (2004) PS1 activates PI3K thus inhibiting GSK-3 activity and tau overphosphorylation: effects of FAD mutations. *EMBO J* 23:2586–2596. <https://doi.org/10.1038/sj.emboj.7600251>
- Bansal N, Yadav P, Kumar M (2017) Ellagic acid administration negated the development of streptozotocin-induced memory deficit in rats. *Drug Res (Stuttg)* 67:425–431. <https://doi.org/10.1055/s-0043-108552>
- Bedse G, Di Domenico F, Serviddio G, Cassano T (2015) Aberrant insulin signaling in Alzheimer's disease: current knowledge. *Front Neurosci* 9:204. <https://doi.org/10.3389/fnins.2015.00204>
- Calsolaro V, Edison P (2016) Neuroinflammation in Alzheimer's disease: current evidence and future directions. *Alzheimers Dement* 12:719–732. <https://doi.org/10.1016/j.jalz.2016.02.010>
- Chen HT, Ruan NY, Chen JC, Lin TY (2012) Dopamine D2 receptor-mediated Akt/PKB signalling: initiation by the D2S receptor and role in quinpirole-induced behavioural activation. *ASN Neuro* 4:371–382. <https://doi.org/10.1042/AN20120013>
- Claiborne A (1985) Catalase activity. In: Greenwald RA (ed) *CRC handbook of methods for oxygen radical research*, 3rd edn. CRC, Boca Raton, pp 283–284
- Ding Y, Zhang B, Zhou K, Chen M, Wang M, Jia Y, Song Y, Li Y, Wen A (2014) Dietary ellagic acid improves oxidant-induced endothelial dysfunction and atherosclerosis: role of Nrf2 activation. *Int J Cardiol* 175:508–514. <https://doi.org/10.1016/j.ijcard.2014.06.045>
- Doens D, Fernandez PL (2014) Microglia receptors and their implications in the response to amyloid  $\beta$  for Alzheimer's disease pathogenesis. *J Neuroinflammation* 11:48. <https://doi.org/10.1186/1742-2094-11-48>
- Ellman GL (1959) Tissue sulfhydryl groups. *Arch Biochem Biophys* 82:70–77
- Ellman GL, Courtney KD, VJr A, Feather-Stone RM (1961) A new and rapid colorimetric determination of acetylcholinesterase activity. *Biochem Pharmacol* 7:88–95
- Ferreira-Vieira TH, Guimaraes IM, Silva FR, Ribeiro FM (2016) Alzheimer's disease: targeting the cholinergic system. *Curr Neuropharmacol* 14:101–115. <https://doi.org/10.2174/1570159X13666150716165726>
- Franke TF (2008) PI3K/Akt: getting it right matters. *Oncogene* 27:6473–6488. <https://doi.org/10.1038/onc.2008.313>
- Gao C, Liu Y, Jiang Y, Ding J, Li L (2014) Geniposide ameliorates learning memory deficits, reduces tau phosphorylation and decreases apoptosis via GSK3 $\beta$  pathway in streptozotocin-induced Alzheimer rat model. *Brain Pathol* 24:261–269. <https://doi.org/10.1111/bpa.12116>
- Guha M, Mackman N (2002) The phosphatidylinositol 3-kinase-Akt pathway limits lipopolysaccharide activation of signaling pathways and expression of inflammatory mediators in human monocytic cells. *J Biol Chem* 277:32124–32132. <https://doi.org/10.1074/jbc.M203298200>
- Harry GJ, Sills R, Schlosser MJ, Maier WE (2001) Neurodegeneration and glia response in rat hippocampus following nitro-L-arginine methyl ester (L-NAME). *Neurotox Res* 3:307–319
- Horecker BL, Komberg A (1948) The extinction coefficient of the reduced band of pyridine nucleotides. *J Biol Chem* 175:385–390
- Kiasalari Z, Heydarifard R, Khalili M, Afshin-Majd S, Baluchnejadmojarad T, Zahedi E, Sanaierad A, Roghani M (2017) Ellagic acid ameliorates learning and memory deficits in a rat model of Alzheimer's disease: an exploration of underlying mechanisms. *Psychopharmacology* 234:1841–1852. <https://doi.org/10.1007/s00213-017-4589-6>
- Kong J, Ren G, Jia N, Wang Y, Zhang H, Zhang W, Chen B, Cao Y (2013) Effects of nicorandil in neuroprotective activation of PI3K/AKT pathways in a cellular model of Alzheimer's disease. *Eur Neurol* 70:233–241. <https://doi.org/10.1159/000351247>
- Landete JM (2011) Ellagitannins, ellagic acid and their derived metabolites: a review about source, metabolism, functions and health. *Food Res Int* 44:1150–1160. <https://doi.org/10.1016/j.foodres.2011.04.027>
- Lee HJ, Ryu JM, Jung YH, Lee SJ, Kim JY, Lee SH, Hwang IK, Seong JK, Han HJ (2016) High glucose upregulates BACE1-mediated A $\beta$  production through ROS-dependent HIF-1 $\alpha$  and LXR $\alpha$ /ABCA1-regulated lipid raft reorganization in SK-N-MC cells. *Sci Rep* 6:36746. <https://doi.org/10.1038/srep36746>
- Li ST, Pan J, Hua XM, Liu H, Shen S, Liu JF, Li B, Tao BB, Ge XL, Wang XH, Shi JH, Wang XQ (2014) Endothelial nitric oxide synthase protects neurons against ischemic injury through regulation of brain-derived neurotrophic factor expression. *CNS Neurosci Ther* 20:154–164. <https://doi.org/10.1111/cns.12182>
- Lipinska L, Klewicka E, Sojka M (2014) The structure, occurrence and biological activity of ellagitannins: a general review. *Acta Sci Pol Technol Aliment* 13:289–299
- Lowry OH, Rosebrough NJ, Farr AL, Randall RJ (1951) Protein measurement with the Folin phenol reagent. *J Biol Chem* 193:265–275
- Mansouri MT, Farbood Y, Naghizadeh B, Shabani S, Mirshekar MA, Sarkaki A (2016) Beneficial effects of ellagic acid against animal models of scopolamine- and diazepam-induced cognitive impairments. *Pharm Biol* 54:1947–1953. <https://doi.org/10.3109/13880209.2015.1137601>
- Meng Y, Wang W, Kang J, Wang X, Sun L (2017) Role of the PI3K/AKT signalling pathway in apoptotic cell death in the cerebral cortex of streptozotocin-induced diabetic rats. *Exp Ther Med* 13:2417–2422. <https://doi.org/10.3892/etm.2017.4259>
- Mohan S, Wu CC, Shin S, Fung HL (2012) Continuous exposure to L-arginine induces oxidative stress and physiological tolerance in cultured human endothelial cells. *Amino Acids* 43:1179–1188. <https://doi.org/10.1007/s00726-011-1173-y>
- Moosavi M, Abbasi L, Zarifkar A, Rastegar K (2014) The role of nitric oxide in spatial memory stages, hippocampal ERK and CaMKII phosphorylation. *Pharmacol Biochem Behav* 122:164–172. <https://doi.org/10.1016/j.pbb.2014.03.021>
- Morris RGM (1984) Development of a water-maze procedure for studying spatial learning in the rats. *J Neurosci Methods* 11:47–60
- Murphy MP (1999) Nitric oxide and cell death. *Biochim Biophys Acta* 1411:401–414
- Ohkawa H, Ohishi N, Yagi K (1979) Assay for lipid peroxides in animal tissues by thiobarbituric acid reaction. *Anal Biochem* 95:351–358
- Ou HC, Lee WJ, Lee SD, Huang CY, Chiu TH, Tsai KL, Hsu WC, Sheu WH (2010) Ellagic acid protects endothelial cells from oxidized low-density lipoprotein-induced apoptosis by modulating the PI3K/Akt/eNOS pathway. *Toxicol Appl Pharmacol* 248:134–143. <https://doi.org/10.1016/j.taap.2010.07.025>
- Paul V, Ekambaram P (2011) Involvement of nitric oxide in learning & memory processes. *Indian J Med Res* 133:471–478
- Paxinos G, Watson CR, Emson PC (1980) AChE-stained horizontal sections of the rat brain in stereotaxic coordinates. *J Neurosci Methods* 3:129–149
- Petanceska SS, Gandy S (1999) The phosphatidylinositol 3-kinase inhibitor wortmannin alters the metabolism of the Alzheimer's amyloid precursor protein. *J Neurochem* 73:2316–2320

- Prast H, Fischer H, Werner E, Werner-Felmayer G, Philippu A (1995) Nitric oxide modulates the release of acetylcholine in the ventral striatum of the freely moving rat. *Naunyn Schmiedeberg's Arch Pharmacol* 352:67–73
- Provias J, Jeynes B (2008) Neurofibrillary tangles and senile plaques in Alzheimer's brains are associated with reduced capillary expression of vascular endothelial growth factor and endothelial nitric oxide synthase. *Curr Neurovasc Res* 5:199–205. <https://doi.org/10.2174/156720208785425729>
- Rajasekar N, Nath C, Hanif K, Shukla R (2017) Intranasal insulin improves cerebral blood flow, Nrf-2 expression and BDNF in STZ (ICV)-induced memory impaired rats. *Life Sci* 173:1–10. <https://doi.org/10.1016/j.lfs.2016.09.020>
- Resende RR, Adhikari A (2009) Cholinergic receptor pathways involved in apoptosis, cell proliferation and neuronal differentiation. *Cell Commun Signal* 7:20. <https://doi.org/10.1186/1478-811X-7-20>
- Rickard NS, Gibbs ME, Ng KT (1999) Inhibition of the endothelial isoform of nitric oxide synthase impairs long-term memory formation in the chick. *Learn Mem* 6:458–466
- Sastry KV, Moudgal RP, Mohan J, Tyagi JS, Rao GS (2002) Spectrophotometric determination of serum nitrite and nitrate by copper-cadmium alloy. *Anal Biochem* 306:79–82
- Sharma N, Deshmukh R, Bedi KL (2010) SP600125, a competitive inhibitor of JNK attenuates streptozotocin induced neurocognitive deficit and oxidative stress in rats. *Pharmacol Biochem Behav* 96:386–394. <https://doi.org/10.1016/j.pbb.2010.06.010>
- Son H, Hawkins RD, Martin K, Kiebler M, Huang PL, Fishman MC, Kandel ER (1996) Long-term potentiation is reduced in mice that are doubly mutant in endothelial and neuronal nitric oxide synthase. *Cell* 87:1015–1023
- Traystman RJ, Moore LE, Helfaer MA, Davis S, Banasiak K, Williams M, Hurn PD (1995) Nitro-L-arginine analogues. Dose- and time-related nitric oxide synthase inhibition in brain. *Stroke* 26:864–869
- Tyagi E, Agrawal R, Nath C, Shukla R (2010) Cholinergic protection via alpha7 nicotinic acetylcholine receptors and PI3K-Akt pathway in LPS-induced neuroinflammation. *Neurochem Int* 56:135–142. <https://doi.org/10.1016/j.neuint.2009.09.011>
- Utkan T, Yazir Y, Karson A, Bayramgurler D (2015) Etanercept improves cognitive performance and increases eNOS and BDNF expression during experimental vascular dementia in streptozotocin-induced diabetes. *Curr Neurovasc Res* 12:135–146. <https://doi.org/10.2174/1567202612666150311111340>
- Vivanco I, Sawyers CL (2002) The phosphatidylinositol 3-kinase AKT pathway in human cancer. *Nat Rev Cancer* 2:489–501. <https://doi.org/10.1038/nrc839>
- Vorhees CV, Williams MT (2006) Morris water maze: procedures for assessing spatial and related forms of learning and memory. *Nat Protoc* 1:848–858
- Winterbourn CC, Hawkins RE, Brian M, Carrell RW (1975) The estimation of red cell superoxide dismutase activity. *J Lab Clin Med* 85:337–341
- Yang Y, Ma D, Xu W, Chen F, Du T, Yue W, Shao S, Yuan G (2016) Exendin-4 reduces tau hyperphosphorylation in type 2 diabetic rats via increasing brain insulin level. *Mol Cell Neurosci* 70:68–75. <https://doi.org/10.1016/j.mcn.2015.10.005>
- Yoshida T, Amakura Y, Yoshimura M (2010) Structural features and biological properties of ellagitannins in some plant families of the order Myrtales. *Int J Mol Sci* 11:79–106. <https://doi.org/10.3390/ijms11010079>
- Zhao Y, Hu X, Liu Y, Dong S, Wen Z, He W, Zhang S, Huang Q, Shi M (2017) ROS signaling under metabolic stress: cross-talk between AMPK and AKT pathway. *Mol Cancer* 16:79. <https://doi.org/10.1186/s12943-017-0648-1>